ACS OMEGA

Open Access

http://pubs.acs.org/journal/acsodf

Article

Effect of Degradation on the Physicochemical and Mechanical Properties of Extruded Films of Poly(lactic acid) and Chitosan

José Ramón Flores-León, Dora Evelia Rodríguez-Félix,* Jesús Manuel Quiroz-Castillo, Heidy Burrola-Núñez, María Mónica Castillo-Ortega, José Carmelo Encinas-Encinas, Juana Alvarado-Ibarra, Hisila Santacruz-Ortega, Jesús Leobardo Valenzuela-García, and Pedro Jesús Herrera-Franco

Cite This: *ACS Omega* 2024, 9, 9526−9535

Read Online

ACCESS | Metrics & More | Article Recommendations

ABSTRACT: This study addresses the fabrication of extruded films using poly(lactic acid) (PLA) and chitosan, with and without maleic anhydride as a compatibilizing agent, for potential applications in disposable food packaging. These films underwent controlled conditions of UV irradiation, water condensation, and temperature variations in an accelerated weathering chamber. The investigation analyzed the effect of different exposure periods on the structural, morphological, mechanical, and thermal properties of the films. It was observed that PLA films exhibited a lower susceptibility to degradation compared to those containing chitosan. Specifically, the pure PLA film showed an increase in elastic modulus and strength during the initial 144 h of exposure, associated with cross-linking induced by UV radiation. On the other hand, film Q2 composed of PLA, chitosan, and maleic anhydride and Q1 without maleic anhydride experienced a tensile strength loss of over 50% after 244 h of exposure. The Q2 film exhibited greater homogeneity, leading to increased resistance to degradation compared to that of Q1. As the degradation time increased, both the Q1 and Q2 films demonstrated a decline in thermal stability. These films also exhibited alterations in crystallinity attributed to the chemo-crystallization process, along with fluctuations in the glass transition temperature and crystallization, particularly at 288 h.

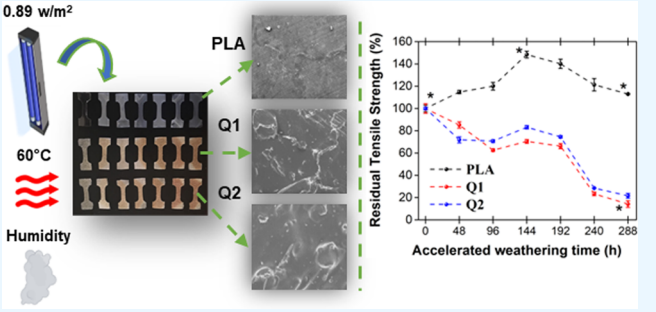

1. INTRODUCTION

The escalating demand for plastic products, predominantly of synthetic origin, has led to concerning accumulation of waste in the environment. The production of food packaging and the widespread use of protective films in agriculture stand out as the primary contributors to this surge in plastic waste.[1−4] Addressing the environmental repercussions of such waste necessitates the exploration of novel materials capable of degrading rapidly under ambient conditions, unlike the protracted degradation periods associated with conventional polymers.[5,6]

Although the integration of natural polymers and/or biopolymers into blends with synthetic polymers has been a common strategy to enhance properties and reduce degradation times, the 88% presence of synthetic polymers may pose environmental challenges during degradation. Therefore, the exclusive use of materials based solely on natural polymers or biopolymers becomes significant, offering the potential to reduce the environmental footprint.[7,8]

Poly(lactic acid) (PLA), a biodegradable and biocompatible polymer with mechanical properties akin to poly(ethylene terephthalate), emerges as a promising candidate for applications in disposable food packaging.[8] Derived from renewable resources such as starch, PLA has a short shelf life and is compatible with food and beverages, making it ideal for applications like disposable packaging and agricultural mulch.[9−11] On the other hand, chitosan is a cationic polysaccharide obtained through the deacetylation of chitin, the second most abundant natural polymer in nature.[12] Chitosan, composed of 2-acetoamido-2-deoxy-D-glucopyrinose and 2-amino-2-deoxy-D-glucopyrinose linked by β (1 → 4) bonds, is characterized by being biodegradable and nontoxic to humans. Additionally, it possesses a high antimicrobial power attributed to the presence of the amino group in the glycosidic

Received: November 21, 2023
Revised: January 24, 2024
Accepted: January 31, 2024
Published: February 13, 2024

ring.[13,14] This biopolymer exhibits susceptibility to different degrading agents, such as solar ultraviolet radiation, environmental humidity, and degradation through the action of microorganisms.[15]

Polymer degradation studies in nature are complex and time-consuming. Therefore, various alternatives have been sought to understand the physicochemical behavior of a material during its degradation but in shorter periods. In this regard, the use of accelerated degradation chambers is an excellent option to study the polymer degradation process. It allows simulating environmental conditions such as UV radiation, temperature, and humidity while intensifying them to obtain faster results.[15] Research focused on studying the effect of chitosan on the degradation of composite materials has been reported. Huerta et al. (2015) explored the degradative behavior of PET/PLA and PET/chitosan films. Accelerated weathering tests indicated that the interaction between PET and chitosan favored the degradation rate compared to the PET/PLA mixture.[10] Similarly, Lizárraga-Laborín et al. studied the degradative behavior of biodegradable films based on polyethylene, PLA, and chitosan. It was observed that the presence of chitosan favored the degradation of the material, with chitosan being the initial component that showed cracking during the degradation process.[16]

In this context, our study undertakes a comprehensive analysis of degradation-induced changes in extruded films of PLA and chitosan subjected to accelerated weathering conditions. We conducted a systematic study to assess the impact of different exposure periods on the physicochemical and mechanical properties of these biopolymer-based films. This research not only advances our understanding of degradation dynamics in such composite materials but also contributes to the development of sustainable alternatives with reduced degradation times, a critical advancement toward mitigating environmental concerns associated with plastic waste.

2. EXPERIMENTAL SECTION

2.1. Materials. Chitosan with a medium molecular weight (190,000−310,000 Da, 75−85% deacetylation) and maleic anhydride (MA) powder, 95% purity (molecular weight of 98.06 g/mol), were obtained from Sigma-Aldrich. Commercial PLA pellets (grade 2003d) with a molecular weight (Mw) of 120,000 Da, specified with a melt flow rate of 6.0 g/10 min (measured at 210 °C with a 2.16 kg load) and a density of 1.24 g/cm^3, was sourced from NatureWorks. Chitosan and PLA were dried at 60 °C for 24 h before use, and MA was used as received.

2.2. Preparation of Extruded Films of PLA and Chitosan. To prepare the composite films, PLA pellets and chitosan were initially ground by using an MF 10 basic mill at 3000 rpm. PLA, chitosan, and MA were individually weighed, and mixtures were then prepared at different weight proportions, as specified in Table 1. Subsequently, the mixtures were homogenized by agitating them with a Booster electric mixer JJ-1 for 15 min through mechanical stirring. Following this, the polymer blends underwent further processing through extrusion molding. This was achieved using an Atlas laboratory mixer-extruder operating at 32 rpm and maintained at specific temperatures of 160 °C for the barrel and 170 °C for the dye.

Table 1. Concentration of Each Component in the Extruded Films

ID	PLA (wt %)	chitosan (wt %)	maleic anhydride (wt %)
PLA	100	0	0
Q1	90	10	0
Q2	89.75	10	0.25

2.3. Accelerated Degradation Studies. PLA, Q1, and Q2 films underwent accelerated degradation by using the Q-Lab QUV/se equipment, which includes UV exposure, water condensation, and irradiation control. Film degradation was analyzed at six different exposure time intervals (Table 2) following the conditions recommended by the ASTM 154 standard. This procedure involved two steps: (1) 8 h of UV irradiation using four 0.89 W/m^2 lamps at 60 °C and (2) 4 h of water condensation at 40 °C.

Table 2. Exposure Time for the Accelerated Degradation of Films

ID	exposure time (h)
T0	0
T1	48
T2	96
T3	144
T4	192
T5	240
T6	288

2.4. Characterization. *2.4.1. Fourier Transform Infrared Spectroscopy (FTIR).* The films exposed to different degradation times were characterized by infrared spectroscopy to investigate the progression of degradation through the potential changes in the chemical structure of the polymers. This analysis was carried out using a Nicolet FTIR spectrophotometer in the ATR mode, over a frequency range from 4000 to 400 cm^{-1}, with an average of 32 scans.

2.4.2. Tensile Strength Test. The mechanical properties of the films were performed on a United SSTM-5kN universal machine equipped with a 5 kN load cell at a constant crosshead speed of 1 mm/min and a jaw spacing of 20 mm. The thickness of the films was determined with a Mitutoyo micrometer, and the dimensions were maintained in a range of 0.3 and 0.6 mm thickness and a width of 5.2 mm. An average of 10 specimens for each test is reported.

2.4.3. Scanning Electron Microscopy (SEM). The effect of the different degradation times on the film morphology was studied by SEM using a scanning electron microscope (JEOL JSM-5410LV) operating at 20 kV. The instrument was equipped with an INCA system and an energy-dispersive X-ray detector (Oxford Instrument). Samples were placed in copper sample holders using double-sided carbon tape and underwent a gold-plating process before analysis.

2.4.4. Thermogravimetric Analysis (TGA). The thermal stability of the films was determined by TGA using a PerkinElmer Pyris 1 TGA unit and a porcelain sample holder. Approximately 4 mg of each sample was weighed and heated within a temperature range from 27 to 600 °C at a heating rate of 10 °C/min in a nitrogen atmosphere. The residual material from the sample holder was then further heated to 900 °C at a rate of 50 °C/min under an oxygen atmosphere to eliminate any remaining residues.

2.4.5. Differential Scanning Calorimetry (DSC). The thermal properties of the films were studied through DSC

https://doi.org/10.1021/acsomega.3c09296
ACS Omega 2024, 9, 9526−9535

using a PerkinElmer DSC 8500 analyzer. The initial heating was conducted at a rate of 10 °C/min, ranging from 0 to 200 °C, in a nitrogen atmosphere (flow rate of 20 mL/min). Following this, the samples underwent a cooling cycle and a second heating cycle under the same conditions as described above. The data obtained from the second heating were analyzed using the Pyris Manager Ink software.

3. RESULTS AND DISCUSSION

3.1. Macroscopic Characteristics of Extruded PLA/Chitosan Films. Extruded films were obtained using polymer mixtures of PLA/chitosan with and without MA, according to the compositions detailed in Table 1. The resulting films from pure PLA exhibited transparency, were colorless, and displayed homogeneity, while films from the polymeric mixture (Q1-Q2) presented a subtle yellow hue characteristic of chitosan particles, which were distributed in the PLA matrix (Figure 1). In general, the films obtained had dimensions of approximately 5.2 mm in width and 0.5 mm in thickness.

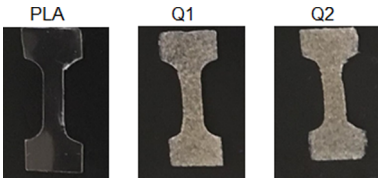

Figure 1. Digital images of the extruded films.

3.2. Accelerated Degradation Study. Figure 2 shows digital images of the extruded films exposed to different degradation times (T0−T6). As observed, the original PLA film (T0) presented a high degree of transparency due to its semicrystalline nature. However, with the extended exposure time, the film transitioned to an opaquer state, possibly due to an increase in crystallinity.[17,18] This change persisted until the 288 h exposure mark. On the other hand, films Q1 and Q2 displayed notable alterations in color as the degradation time increased, undergoing a gradual shift from the initial yellow color to a darker orange hue. According to existing literature, these changes are related to the appearance of chromophore functional groups induced by radiation exposure.[19] Additionally, isolated cracks were observed in the Q1 film after 240 h with a more pronounced manifestation during the final exposure time (T6). On the contrary, the Q2 film, which incorporates a compatibilizer, exhibited fewer and smaller cracks throughout the 288 h of degradation period, suggesting that the presence of MA confers some degree of resistance to degradation.

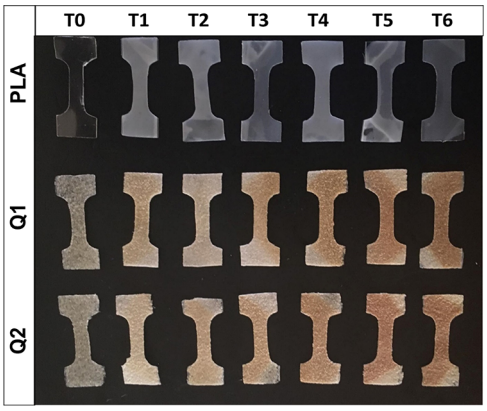

Figure 2. Digital images of the films corresponding to the different periods of exposure to accelerated degradation.

3.2.1. Fourier Transform Infrared Analysis (FTIR). Figure 3 shows the infrared spectra for each of the pure components.

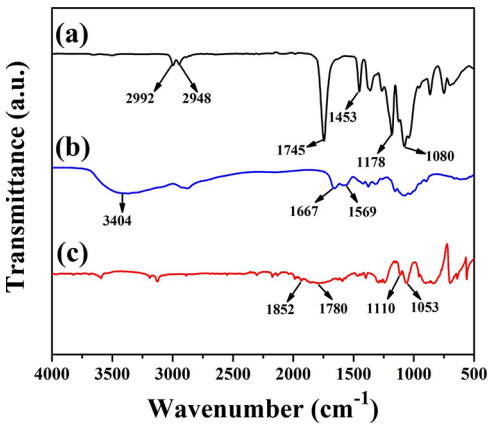

Figure 3. Infrared spectra of the pure components: (a) PLA, (b) chitosan, and (c) MA.

PLA showed the characteristic signals of the ester functional group; in this way the stretching of the carbonyl group (C═O) appears at 1745 cm^{-1} and the asymmetric and symmetric stretching of the C−O−C bond at 1178 and 1080 cm^{-1}, respectively. In addition, the signals corresponding to the asymmetric and symmetric stretching of the methyl group ($-CH_3$) appear at 2992 and 2948 cm^{-1} and the asymmetric and symmetric bending of this group at 1453 and 1363 cm^{-1}, respectively.[20,21] The chitosan spectrum showed the characteristic signals of hydroxyl group stretching (−OH) at 3404 cm^{-1}, amide-II (NH) bending at 1667 cm^{-1}, and amine (NH_2) twisting at 1569 cm^{-1}. On the other hand, the MA spectrum showed the signals attributed to the asymmetric and symmetric stretching of the carbonyl group at 1852 and 1780 cm^{-1}, respectively, as well as the asymmetric and symmetric stretching of the C−O−C bonds at 1110 and 1053 cm^{-1}, respectively.[22]

Figure 4 shows the infrared spectra corresponding to the PLA films Q1 and Q2 exposed to different degradation times. The spectrum of the PLA film (Figure 4b) presented a new peak at around 895 cm^{-1} after 240 h of exposure. This signal is attributed to the symmetric bending of a double bond in acrylate residues resulting from the Norrish type II photodegradation of the polymer (Figure 5a).[23,24] On the contrary, it proved challenging to identify other changes in the infrared spectrum associated with alternative degradation mechanisms, possibly due to this film's pronounced resistance to degradation. On the other hand, the Q1 film (Figure 4c) displayed a new peak around 3412 cm^{-1} at 240 h of exposure, which can be attributed to the stretching of the hydroxyl (OH) group, associated with chitosan hydrolysis within the film (Figure 5b).[25] As observed, this peak showed both a shift to a higher wavenumber and an increase in intensity during the final degradation time (T6), indicating a higher degree of hydrolysis and, consequently, a greater degradation of the film.[26] Additionally, similar to the PLA, this film presented a peak around 895 cm^{-1} at 144 and 192 h of exposure (Figure

https://doi.org/10.1021/acsomega.3c09296
ACS Omega 2024, 9, 9526−9535

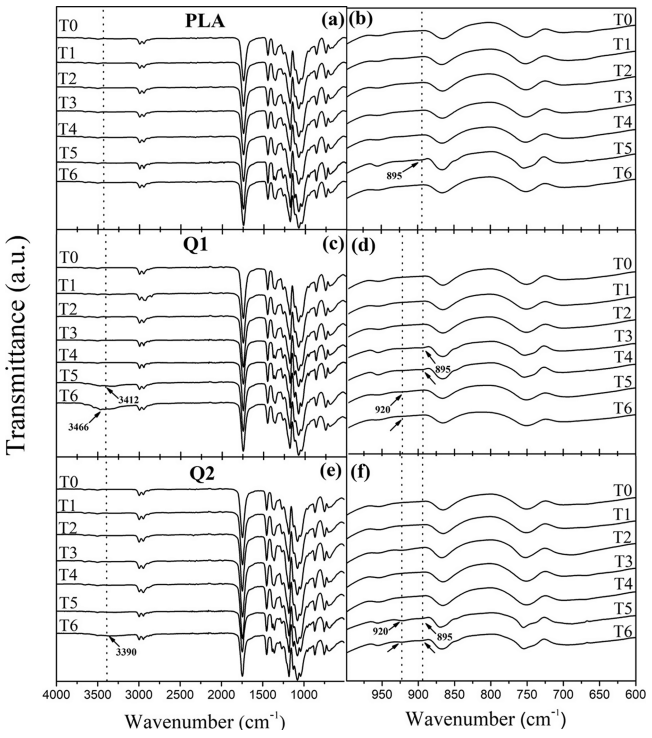

Figure 4. Infrared spectra of (a,b) PLA, (c,d) Q1, and (e,f) Q2 films at different exposure times of accelerated weathering.

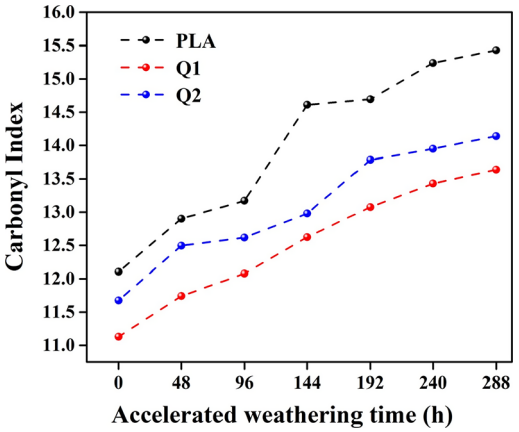

Figure 6. Carbonyl index of films at different exposure times.

4d). Furthermore, during the latter two times T5-T6, another new signal was observed at 920 cm^{-1}, which is attributed to the asymmetric bending of double bonds, as previously mentioned, is associated with the photodegradation of the PLA within the composite film.[24−27] Finally, similar to Q1, the Q2 film exhibited the peak associated with hydrolysis at 3390 cm^{-1}; however, this peak only appeared after 288 h of degradation (Figure 4e). Its appearance during the final degradation period (T6) may indicate the higher resistance of this film to the degradation process.

At present, the carbonyl index is the most commonly employed indicator for monitoring the chemical oxidation and degradation of polymers. This choice is substantiated by reports indicating that when polymers are exposed to specific energy source, such as ultraviolet radiation, they can experience photooxidation reactions and subsequent chain breaks.[25−28] Based on the above, the carbonyl index of the analyzed films was determined by calculating the ratio of the integrated absorbance of the carbonyl group band at 1750 cm^{-1} to that of a reference band corresponding to the symmetrical bending of the methyl group at 1453 cm^{-1}, which remains insensitive to photooxidation.[29] Figure 6 illustrates the carbonyl index for the composite films exposed to accelerated degradation. An increase in the carbonyl index was noted for all films as the degradation time was extended, with the highest values recorded at 288 h of exposure. These results confirm the effective photodegradation for each composite film due to the effect of ultraviolet radiation.[30]

3.2.2. Scanning Electron Microscopy. Using SEM, we conducted surface morphology analysis of the films before and after the accelerated degradation process (Figure 7). Prior to exposure to accelerated degradation (T0), the PLA film exhibited a smooth and homogeneous surface. However, upon the introduction of chitosan into the film (Q1), a loss of

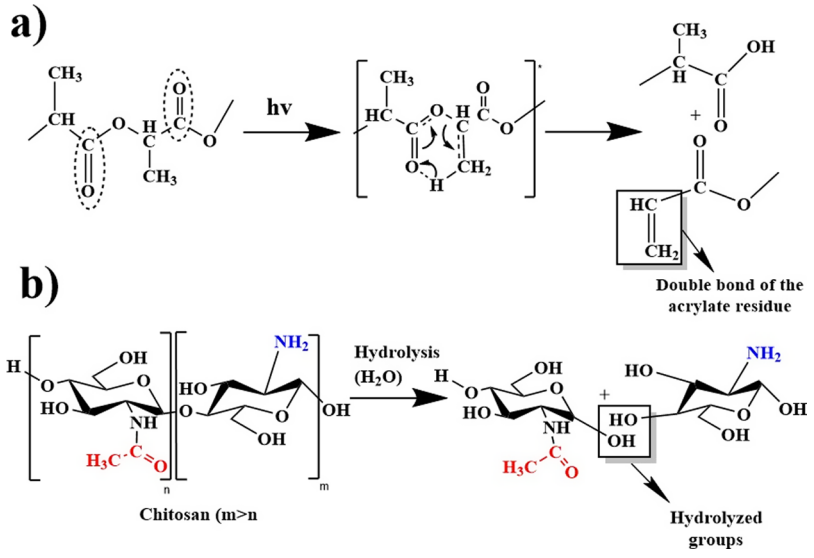

Figure 5. Proposed degradation mechanism for the films: (a) photodegradation of PLA via Norrish II and (b) hydrolysis degradation of chitosan.

https://doi.org/10.1021/acsomega.3c09296
ACS Omega 2024, 9, 9526−9535

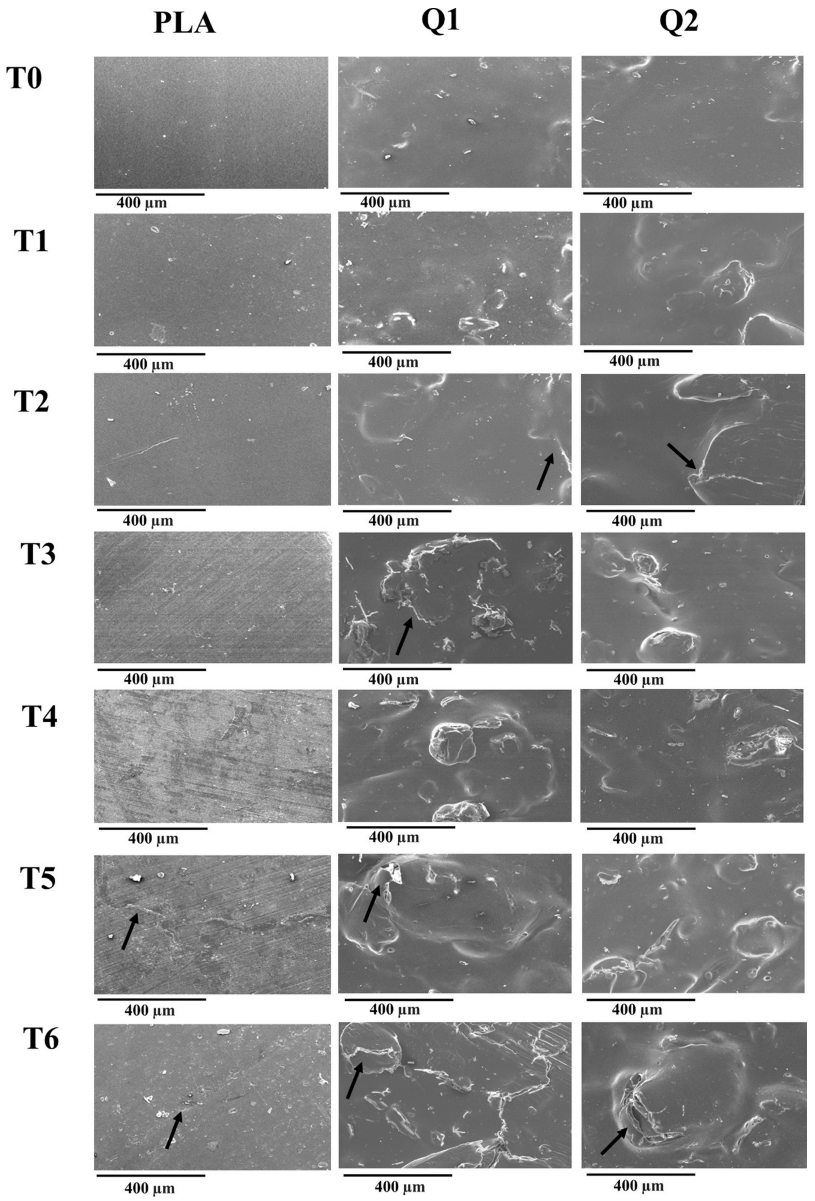

Figure 7. Micrographs of the surface of extruded films subjected to different exposure times of accelerated degradation. 150× magnification, scale bar 400 μm.

homogeneity was observed as chitosan displayed a tendency to form random agglomerates within the system. In contrast, the Q2 film, with MA, displayed improved homogeneity compared to the film without this component, resulting in the reduction of chitosan agglomerates within the PLA matrix. These findings suggest a compatibilizing effect of maleic anhydride in the composite film.[31,32] Furthermore, we observed distinct changes in the morphology of the films during the degradation period. The PLA film exhibited alterations in its surface morphology starting at 192 h (T4), characterized by small isolated cracks. However, at 240 and 288 h (T5 and T6) of exposure, more substantial cracks became evident in specific regions of the material. On the other hand, both the Q1 and Q2 films exhibited crack formation as early as 96 h. Notably, the Q1 film displayed more extensive degradation compared with the Q2 film, showing larger cracks at each degradation time, primarily within the chitosan agglomerates. This observation highlights that reduced chitosan agglomerate formation in the PLA matrix, facilitated by the compatibilizing agent (MA), effectively mitigated material degradation under the given conditions. It is worth emphasizing that the most pronounced degradation effect was consistently observed at the final exposure time (T6) in both films.[33,34]

3.2.3. Residual Mechanical Properties. In Figure 8a, the behavior of the residual elastic modulus (residual Young's modulus) of the films at different exposure times was observed. The PLA film exhibited a gradual and significant increase in this property during the first 144 h, reaching a residual elastic modulus of 155.17%. This behavior can be attributed to cross-linking of the PLA chains due to the effect of ultraviolet radiation, where the formation of new covalent bonds reduces the mobility and flexibility of polymer chains, ultimately increasing the film's rigidity.[35] After 144 h of exposure, a decrease in the elastic modulus was observed. However, it is crucial to highlight that these values turned out to be higher than those of pristine PLA (T0). Specifically, in the last degradation period (288 h), the film exhibited a residual elastic modulus of 111.70%.

https://doi.org/10.1021/acsomega.3c09296
ACS Omega 2024, 9, 9526−9535

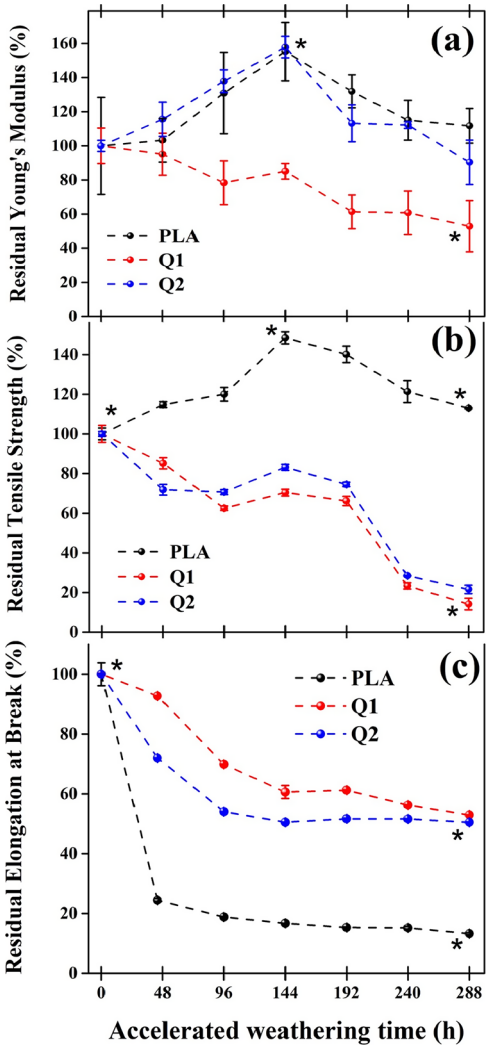

Figure 8. Residual mechanical properties of the films at different exposure times of accelerated degradation. (a) Residual Young's modulus; (b) residual tensile strength; and (c) residual elongation at break. Asterisks indicate significant differences ($P < 0.05$).

Similar to PLA, the Q2 film exhibited consistent behavior, reaching a maximum elastic modulus value of 157.81% at 144 h of exposure and a value of 90.37% at 288 h of exposure. This behavior can be attributed to the homogeneous distribution of chitosan in the PLA matrix, allowing for partial preservation of PLA properties. Q1 film, on the other hand, displayed a significantly different behavior compared to PLA and Q2 films. It exhibited a gradual decrease in the residual elastic modulus from the initial 48 h of exposure, maintaining this trend until the final degradation period (288 h), where it reached a residual modulus of 52.23%. This behavior could be attributed to the accumulation of chitosan at the interface of the polymeric matrix, leading to a reduction in cross-linking between polymer chains and, simultaneously, promoting the narrowing and rupture of the film.

The residual tensile strength analysis is shown in Figure 8b. The PLA film exhibited a gradual increase during the initial 144 h of exposure, reaching a value of 148.43%. This behavior is attributed to the cross-linking in the material, as mentioned earlier. Subsequently, a gradual decrease was observed, presenting a value of 113.45% at 288 h. However, even at this extended exposure time, the strength remains higher compared to the pristine PLA film (T0), suggesting a certain resistance to the degradation process of this film.[36] On the other hand, the Q1 and Q2 films exhibited a continuous decrease in their residual tensile strength from the initial 48 h of exposure. Specifically, both films demonstrated a reduction of over 50% at 240 h, reaching final values of 14.16% for Q1 and 21.58% for Q2 at the end of the degradation period (288 h). When relating the observed behavior in the residual strength analysis to the results obtained through SEM (Figure 7), it is observed that the lower residual strength of the Q1 film is due to a higher presence of cracks associated with chitosan agglomerates within the film. This results in a reduced ability to withstand loads before crack propagation and film rupture. In contrast, the higher residual strength of the Q2 film may be associated with a lower formation of chitosan agglomerates, and consequently, fewer cracks within the film.[37]

In Figure 8c, the residual elongation at fracture is depicted, showing a consistent decrease in this property for all of the films over the course of exposure. Notably, the PLA film exhibited an initial value of 24.42% at 48 h, followed by a gradual decrease, ultimately reaching a residual elongation of 13.80% at 288 h of exposure. This trend aligns with the results obtained for the residual elastic modulus, indicating an increase in the film's rigidity. In contrast, both the Q1 and Q2 films also experienced decreases in their elongation percentages, albeit to a lesser extent when compared to the PLA film. They exhibited values of 52 and 50.25%, respectively, at 288 h of exposure. Overall, the Q2 film displayed lower residual elongation in comparison to the Q1 film, which is consistent with the elastic modulus values observed in both films.

3.2.4. Thermal Analysis. The effect of accelerated degradation time on the thermal stability of the films was investigated by using TGA (Figure 9). In Figure 9a, the thermograms of the PLA films corresponding to each exposure period (T0−T6) are presented. A gradual increase in the inflection temperature was observed during the initial 144 h, reaching a maximum of 360.97 °C. This increase in thermal stability is associated with the enhanced formation of cross-links in the polymeric chains, aligning with the trends observed in the mechanical properties analysis (Figure 8).[35] After 144 h (T3) of exposure, a shift in the inflection temperature trend was observed, with a gradual decrease over time, ultimately reaching a temperature of 352.14 °C after 288 h (T6). This behavior could be linked to the breakage of PLA chains, as proposed in the carbonyl index studies (Figure 6).[38,39] On the other hand, the thermogram corresponding to the Q1 film is presented in Figure 9b. In contrast to the pure PLA film, the Q1 film experienced a decrease in its thermal stability from the first 48 h of exposure, a trend that continued until 288 h (T6), where it exhibited the lowest inflection temperature with a value of 336.26 °C. These results suggest a reduced resistance to degradation in the Q1 film compared to that in PLA, which could be related to the high susceptibility of chitosan to decompose under accelerated degradation conditions.[16,40] Finally, the Q2 film exhibited a lower thermal stability at each of the exposure times compared to the pristine film (Figure 9c). However, some intriguing trends were observed. Specifically, the film displayed an inflection temperature of 341.90 °C at 48 h, which gradually increased to reach its highest value of 352.14 °C at 144 h. This behavior could be associated with the formation of cross-links in the polymeric chains, facilitated by the presence of MA. As the exposure time to radiation increases, MA has the ability to generate radical

https://doi.org/10.1021/acsomega.3c09296
ACS Omega 2024, 9, 9526−9535

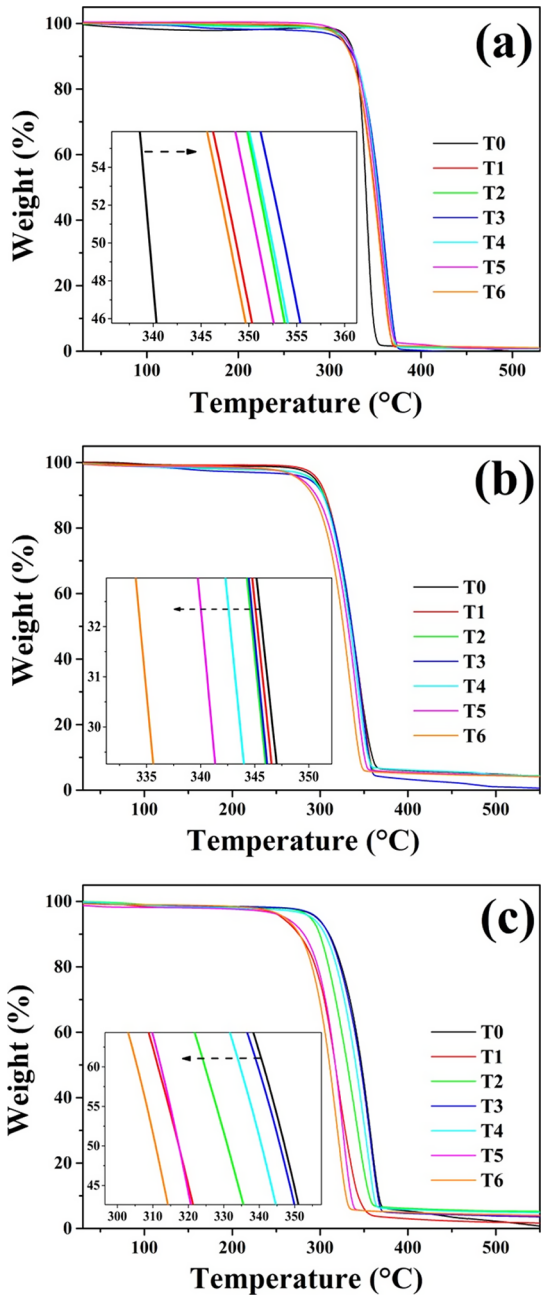

Figure 9. TGA thermograms of the films of (a) PLA, (b) Q1, and (c) Q2 at different exposure times of accelerated degradation.

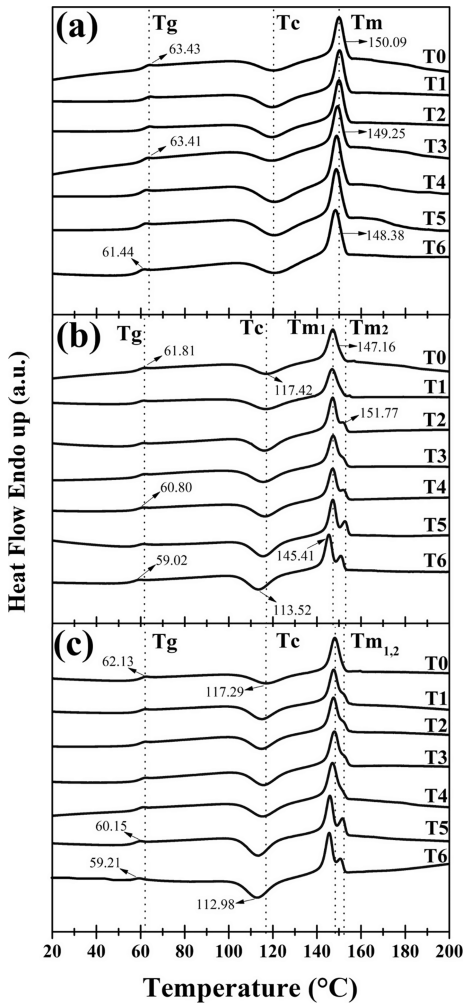

Figure 10. DSC thermograms of (a) PLA, (b) Q1, and (c) Q2 films at different exposure times of accelerated degradation.

species that promote the formation of covalent bonds within the film.[41] However, after 144 h, a decrease in the inflection temperature was observed, reaching a value of 333.84 °C at 288 h, which is related to the degradation of the material due to its exposure in the weathering chamber.

The analysis by DSC of the composite films for each degradation period is depicted in Figure 10. As observed, the glass transition temperature (T_g) and melting temperature (T_m) for the pure PLA film (Figure 10a) remained constant during the first 144 h of degradation. Following this period, the film underwent a gradual decrease, reaching values of 61.44 and 148.38 °C for T_g and T_m, respectively, at 288 h of degradation (T6). This decline could be associated with the photolysis of PLA chains, as observed in the results obtained from FTIR and carbonyl index analyses.[39,42]

On the other hand, the nondegraded Q1 film (T0) exhibited a T_g of 61.81 °C, which remained constant between times T1−T5 (Figure 10b). However, at 288 h (T6) of exposure, corresponding to the last degradation period, a shift to a lower temperature was observed, showing a corresponding T_g value of 59.02 °C. As mentioned earlier, this behavior could be associated with the increased mobility of the polymeric chains, mainly due to the degradation of chitosan in the composite film.[19] Additionally, a decrease in the crystallization temperature (T_c) of the film was observed after the first 48 h, maintaining this trend throughout the rest of the accelerated weathering process (T1−T6). This can be attributed to the rearrangement of the polymeric chains favored by the degradative process under accelerated weathering conditions.

The Q1 film also displayed significant changes in crystallinity percentages (X_c %). The pristine material (T0) had a crystallinity of 39.20% (Table 3), which gradually increased with exposure time, reaching a maximum increase of approximately 6% at 288 h. This behavior is related to the reorganization or migration of degraded amorphous segments into crystalline phases, known as chemo-crystallization and has been reported by various researchers.[43,44] Conversely, the transition assigned to the melting of the material (T_{m1}) occurred at 147.16 °C at T0. Furthermore, at 96 h (T2), the appearance of a second endothermic peak (T_{m2}) at 151.77 °C

https://doi.org/10.1021/acsomega.3c09296
ACS Omega 2024, 9, 9526−9535

Table 3. Crystallinity Percentages of Films Subjected to Different Exposure Times of Accelerated Degradation

	X_c (%)			ΔH_{cc} (J/g)			ΔH_m (J/g)		
accelerated weathering time (h)	PLA	Q1	Q2	PLA	Q1	Q2	PLA	Q1	Q2
0	36.81	39.20	33.90	−13.60	−17.98	−12.89	20.89	18.75	18.84
48	38.14	41.45	39.26	−15.39	−16.98	−15.93	20.34	21.85	20.86
96	38.30	42.31	40.45	−16.56	−18.32	−15.16	19.32	21.32	22.74
144	39.64	43.94	41.57	−18.19	−18.23	−19.02	18.95	22.94	19.95
192	39.90	44.62	41.60	−16.72	−20.13	−17.94	20.63	21.6	21.04
240	39.74	44.33	41.25	−15.90	−17.96	−16.66	21.33	23.31	21.99
288	39.79	45.41	43.26	−13.95	−17.43	−16.17	23.33	25.11	24.37

was observed, gradually increasing in intensity with the exposure time. This could be correlated with the decrease in the crystallization temperature of the film. When crystallization occurs at a lower temperature, fewer perfect crystals are formed, and these can recrystallize at higher temperatures. Thus, the formed crystals (recrystallized) are more stable and contribute to the second T_{m2} transition.[45] Additionally, a gradual decrease in the T_{m1} values was observed with respect to the exposure time, showing a value of 145.41 °C at 288 h. This behavior may indicate a decrease in the molecular weight of the material due to the degradation process. Finally, as shown in Figure 10c, the Q2 film exhibited slight shifts in T_g in the last two degradation times T5−T6. Additionally, similar to the Q1 film, a decrease in the crystallization temperature and a gradual increase in the crystallinity percentages over degradation time were observed, indicating effective degradation of this film.

4. CONCLUSIONS

In conclusion, the successful production of PLA/chitosan films, with and without MA, was achieved through the extrusion molding technique. The presence of chitosan in Q1 films favored the degradative process, evident through crack formation, especially after the initial 96 h (T3) of degradation. Conversely, the addition of MA mitigated this process in the Q2 film, attributed to the reduction of chitosan clusters through compatibilization. All films exhibited an increase in the carbonyl index over the accelerated weathering time, indicative of a photodegradation process. However, the Q1 and Q2 films were notably more affected by humidity conditions, as evidenced by the increased intensity of the hydroxyl group in the infrared spectrum. The incorporation of chitosan significantly affected the mechanical properties, leading to a reduction in tensile strength of over 50% after 244 h of exposure. Nevertheless, the films with MA showed higher values in tensile strength and elastic modulus compared with those without MA (Q1), confirming greater resistance to degradation of the Q2 films. Regarding thermal stability, pure PLA films exhibited an increase in their inflection temperature during the initial 144 h, associated with the cross-linking of their chains due to the effect of UV radiation. In contrast, the Q1 and Q2 films decreased their thermal stability due to the scission of polymeric chains. To summarize, the addition of chitosan significantly influenced the physicochemical and mechanical properties of the composite material during accelerated degradation. These findings provide a valuable foundation for future research, particularly in the development of disposable food packaging.

AUTHOR INFORMATION

Corresponding Author

Dora Evelia Rodríguez-Félix − *Departamento de Investigación en Polímeros y Materiales, Universidad de Sonora, C.P. 83000 Hermosillo, Sonora, Mexico;* orcid.org/0000-0002-3952-9329; Email: dora.rodriguez@unison.mx

Authors

José Ramón Flores-León − *Departamento de Investigación en Polímeros y Materiales, Universidad de Sonora, C.P. 83000 Hermosillo, Sonora, Mexico*

Jesús Manuel Quiroz-Castillo − *Departamento de Investigación en Polímeros y Materiales, Universidad de Sonora, C.P. 83000 Hermosillo, Sonora, Mexico;* orcid.org/0000-0002-8810-6162

Heidy Burrola-Núñez − *Licenciatura de Ecología, Universidad Estatal de Sonora, C.P. 83100 Hermosillo, Sonora, Mexico*

María Mónica Castillo-Ortega − *Departamento de Investigación en Polímeros y Materiales, Universidad de Sonora, C.P. 83000 Hermosillo, Sonora, Mexico*

José Carmelo Encinas-Encinas − *Departamento de Investigación en Polímeros y Materiales, Universidad de Sonora, C.P. 83000 Hermosillo, Sonora, Mexico*

Juana Alvarado-Ibarra − *Departamento de Investigación en Polímeros y Materiales, Universidad de Sonora, C.P. 83000 Hermosillo, Sonora, Mexico*

Hisila Santacruz-Ortega − *Departamento de Investigación en Polímeros y Materiales, Universidad de Sonora, C.P. 83000 Hermosillo, Sonora, Mexico;* orcid.org/0000-0002-7123-8791

Jesús Leobardo Valenzuela-García − *Departamento de Ingeniería Química y Metalurgia, Universidad de Sonora, C.P. 83000 Hermosillo, Sonora, Mexico*

Pedro Jesús Herrera-Franco − *Centro de Investigación Científica de Yucatán, Unidad de Materiales, C.P. 97205 Mérida, Yucatán, Mexico*

Complete contact information is available at: https://pubs.acs.org/10.1021/acsomega.3c09296

Notes

The authors declare no competing financial interest.

ACKNOWLEDGMENTS

J.R.F.-L. acknowledges CONAHCYT (Consejo Nacional de Humanidades, Ciencia y Tecnología, México) for the graduate grant provided for his graduate studies.

https://doi.org/10.1021/acsomega.3c09296
ACS Omega 2024, 9, 9526−9535

REFERENCES

(1) Marsh, K.; Bugusu, B. Food packaging-roles. Materials, and Environmental Issues. *J. Food Sci.* **2007**, *72* (3), 39−55.

(2) Boro, U.; Moholkar, V.-S. Antimicrobial bionanocomposites of poly(lactic acid)/ZnO deposited halloysite nanotubes for potential food packaging applications. *Mater. Today Commun.* **2022**, *33*, No. 104787.

(3) Othman, N.; Selambakkannu, S.; Seko, N. Biodegradable dual-layer Polyhydroxyalkanoate (PHA)/Polycaprolactone (PCL) mulch film for agriculture: Preparation and characterization. *Energy Nexus* **2022**, *8*, No. 100137.

(4) Pereira, D.-F.; Branco, A.-C.; Claudio, R.; Marques, A.-C.; Figueiredo, C.-G. Development of composites of PLA filled with different amounts of rice husk fibers for fused deposition modeling. *J. Nat. Fibers* **2023**, *20* (1), No. 2162183.

(5) Rodríguez, D.-E.; Quiroz, J.-M.; Del Castillo, T.; Castillo, M.-M.; Ramírez, L.-P.; García, D.; Mendívil, T. *Preparation and characterization of degradable composite materials*. Superficies y Vació: 2015; Vol. *28*, No. 1, pp 18−24

(6) Noori, A.; Zadhoush, A.; Bahri, N. Morphology and thermal degradation studies of melt-mixed poly(lactic acid) (PLA)/poly(ε-caprolactone) (PCL) biodegradable polymer blend nanocomposites with TiO2 as filler. *Polym. Test.* **2015**, *45*, 93.

(7) Ding, Y.; Feng, W.; Huang, D.; Lu, B.; Wang, P.; Wang, G.; Ji, J. Compatibilization of immiscible PLA-based biodegradable polymer blends using amphiphilic di-block copolymers. *Eur. Polym. J.* **2019**, *118*, 45−52.

(8) Rasal, R.-M.; Janorkar, A.-V.; Hirt, D.-E. Poly(lactic acid) modifications. *Prog. Polym. Sci.* **2010**, *35* (3), 338−356.

(9) Zhou, H.; Lawrence, J.-G.; Bhaduri, S.-B. Fabrication aspects of PLA-CaP/PLGA-CaP composites for orthopedic applications: A review. *Acta Biomaterialia.* **2012**, *8* (6), 1999−2016.

(10) Torres, A.-M.; Palma, D.; Domínguez, M.-A.; Del Angel, D.; De la Fuente, D. Comparative assessment of miscibility and degradability on PET/PLA and PET/chitosan blends. *Eur. Polym. J.* **2014**, *61*, 285−299.

(11) Vek, M.; Paul, U.-C.; Zia, J.; Mancini, G.; Sedlarik, V.; Athanassiou, A. Biodegradable Films of PLA/PPC and Curcumin as Packaging Materials and Smart Indicators of Food Spoilage. *ACS Appl. Mater. Interfaces* **2022**, *14* (12), 14654−14667.

(12) Shojaee, S.-M.; Mortazavi, S.; Seyfi, J. Preparation and characterization of polyvinyl alcohol/chitosan blends plasticized and compatibilized by glycerol/polyethylene glycol. *Carbohydr. Polym.* **2020**, *232*, No. 115784.

(13) Grande, R.; Pessan, L.-A.; Carvalho, A.-J. Ternary melt blends of poly(lactic acid)/poly(vinyl alcohol)-chitosan. *Industrial Crops and Products.* **2015**, *72*, 159−165.

(14) Wei, L.; Tan, W.; Wang, G.; Li, Q.; Dong, F.; Guo, Z. The antioxidant and antifungal activity of chitosan derivatives bearing Schiff bases and quaternary ammonium salts. *Carbohydr. Polym.* **2019**, *226*, No. 115256.

(15) La Mantia, F.-P.; Morreale, M.-B.; Mistretta, M. C.; Ceraulo, M.; Scaffaro, R. Degradation of polymer blends: A brief review. *Polym. Degrad. Stab.* **2017**, *145*, 79−92.

(16) Lizárraga-Laborín, L.-L.; Quiroz, J.-M.; Encinas, J.-C.; Castillo, M.-M.; Burruel, S.-E.; Romero, J.; Torres, J.-A.; Cabrera, D.; Rodríguez, D.-E. Accelerated weathering study of extruded polyethylene/poly(lactic acid)/chitosan films. *Polym. Degrad. Stab.* **2018**, *155*, 43−51.

(17) Madera, T.-J.; Meléndrez, R.; González, G.; Quintana, P.; Pillai, S.-D. Effect of gamma irradiation on physicochemical properties of commercial poly(lactic acid) clamshell for food packaging. *Radiat. Phys. Chem.* **2016**, *123*, 6−13.

(18) Navarro, I.; Sessini, V.; Dominici, F.; Torre, L.; Kenny, J.-M.; Peponi, L. Design of biodegradable blends based on PLA and PCL: From morphological, thermal and mechanical studies to shape memory behavior. *Polym. Degrad. Stab.* **2016**, *132*, 97−108.

(19) Carlsson, D.-J.; Wiles, D.-M The photooxidative degradation of polypropylene. Part I. Photooxidation and photoinitiation processes. *J. Macromol. Sci., Polym. Rev.* **1976**, *14* (1), 65−106.

(20) Hassan, N.-A.; Ahmad, S.; Chen, R.-S.; Shahdan, D.; Kassim, M.-H. Tailoring lightweight, mechanical and thermal performance of PLA/recycled HDPE biocomposite foams reinforced with kenaf fibre. *Ind. Crops Prod.* **2023**, *197*, No. 116632.

(21) Li, X.; Shang, X.; Lyu, J.; Tong, Y.; Situ, W.; Yu, L.; Wu, T.; Xie, H.; Qu, J. Efficient fabrication of PLA/PHB composites with enhanced mechanical properties, excellent thermal stability, fast crystallization ability, and degradation rate via the synergistic of weak shear field and melt quenching technique. *Ind. Crops Prod.* **2023**, *196*, No. 116516.

(22) Koker, H.-S.; Ersan, H.-Y.; Aytac, A. Effects of PE-g-MA on tensile, thermal, surface, barrier properties, and morphology of plasticized LDPE/chitosan films. *Iran. Polym. J.* **2023**, *32*, 263−273.

(23) Lv, S.; Liu, X.; Gu, J.; Jiang, Y.; Tan, H.; Zhang, Y. Effect of glycerol introduced into PLA based composites on the UV weathering behavior. *Construction and Building Materials.* **2017**, *144*, 525−531.

(24) Chopra, S.; Pande, K.; Puranam, P.; Deshmukh, A.-D.; Bhone, A.; Kale, R.; Galande, A.; Mehtre, B.; Tagad, J.; Tidake, S. Explanation of the mechanism governing atmospheric degradation of 3D-printed poly(lactic acid) (PLA) with different in-fill pattern and varying in-fill density. *RSC Advances.* **2023**, *13*, 7135−7152.

(25) Copinet, A.; Bertrand, C.; Govindin, S.; Coma, V.; Couturier, Y. Effects of ultraviolet light (315 nm), temperature and relative humidity on the degradation of polylactic acid plastic films. *Chemosphere.* **2004**, *55* (5), 763−773.

(26) Ghasemlou, M.; Daver, F.; Murdoch, B.-J.; Ball, A.-S.; Ivanova, E.-P.; Adhikari, B. Biodegradation of novel bioplastics made of starch, polyhydroxyurethanes, and cellulose nanocrystals in the soil environment. *Sci. Total Environ.* **2022**, *815*, No. 152684.

(27) Tsai, M.-H.; Ouyang, H.; Yang, F.; Wei, M.-K.; Lee, S. Effects of ultraviolet irradiation on the aging of poly(lactic acid)/methyl methacrylate blends. *Polymer* **2022**, *252*, No. 124947.

(28) Gulmine, J.-V.; Akcelrud, L. Correlations between structure and accelerated artificial ageing of XLPE. *Eur. Polym. J.* **2006**, *42* (3), 553−562.

(29) Rouillon, C.; Bussiere, P.-O.; Desnoux, E.; Collin, S.; Vial, C.; Therias, S.; Gardette, J.-L. Is carbonyl index a quantitative probe to monitor polypropylene photodegradation? *Polym. Degrad. Stab.* **2016**, *128*, 200−208.

(30) Zhou, Q.; Liu, X.; Lu, Y.; Dao, X.; Qiu, L. Accelerated Laboratory Weathering of Polypropylene/Poly(Lactic Acid) Blends. *Polymers.* **2023**, *15* (1), 17.

(31) Bernardo, M.-P.; Rodrigues, B.-C.; Sechi, A.; Mattoso, L.-H. Grafting of maleic anhydride on poly (lactic acid)/hydroxyapatite composites augments their ability to support osteogenic differentiation of human mesenchymal stem cells. *Journal of Biomaterials Applications.* **2023**, *37* (7), 1286−1299.

(32) Ye, G.; Li, Z.; Chen, B.; Bai, X.; Chen, X.; Hu, Y. Performance of polylactic acid/polycaprolactone/microcrystalline cellulose biocomposites with different filler contents and maleic anhydride compatibilization. *Polym. Compos.* **2022**, *43* (8), 5179−5188.

(33) Ganesan, C.; Chandrasekar, M.; Nisha, M. S.; Subha, S.; Muthukumar, C.; Krishnasamy, S.; Thiagamani, S. M. K.; Siengchin, S.; Ganesan, C.; Chandrasekar, M.; Nisha, M.-S.; Subha, S. Effect of Compatibilizer on the Aging and Degradation Mechanism of the Natural Fiber-Reinforced Thermoplastic Composites. In *Advances in Materials and Metallurgy*; 2022; pp 1−15.

(34) Martín del Campo, A.-S.; Robledo, J.-R.; Arellano, M.; Rabelero, M.; Pérez, A.-A. Accelerated Weathering of Polylactic Acid/Agave Fiber Biocomposites and the Effect of Fiber-Matrix Adhesion. *J. Polym. Environ.* **2020**, *29*, 937−947.

(35) Tsuji, H.; Sugiyama, H.; Sato, Y. Photodegradation of Poly (lactic acid) Stereocomplex by UV-Irradiation. *Journal of Polymers and the Environment.* **2012**, *20* (3), 706−712.

(36) Scaffaro, R.; Maio, A.; Gammino, M.; La Mantia, F.-P. Effect of an organoclay on the photochemical transformations of a PBAT/PLA

https://doi.org/10.1021/acsomega.3c09296
ACS Omega 2024, 9, 9526−9535

blend and morpho-chemical features of crosslinked networks. *Polym. Degrad. Stab.* **2021**, *187*, No. 109549.
(37) Spiridon, I.; Paduraru, O.-M.; Zaltariov, M.-F.; Darie, R.-N. Influence of Keratin on Polylactic Acid/Chitosan Composite Properties. Behavior upon Accelerated Weathering. *Ind. Eng. Chem. Res.* **2013**, *52* (29), 9822−9833.
(38) Amato, P.; Muscetta, M.; Venezia, V.; Cocca, M.; Gentile, G.; Castaldo, R.; Marotta, R.; Vitiello, G. Eco-sustainable design of humic acids doped ZnO nanoparticles for UVA/light photocatalytic degradation of LLDPE and PLA plastics. *J. Environ. Chem. Eng.* **2023**, *11* (1), No. 109003.
(39) Laongdaw, T.; Suchart, S.; Rapeephun, D.; Jyotishkumar, P. Influence of accelerated weathering on the thermo-mechanical, antibacterial, and rheological properties of polylactic acid incorporated with porous silica-containing varying amount of capsicum oleoresin. *Composites, Part B* **2019**, *175*, No. 107108.
(40) Afkhami, A.; Rezaei, M.; Jafarizadeh, H. Effect of chitosan incorporation on crystallinity, mechanical and rheological properties, and photodegradability of PE/TPS blends. *J. Thermoplast. Compos. Mater.* **2019**, *34* (6), No. 089270571985449.
(41) Zhao, H.; Xi, C.; Zhao, X.-D.; Sun, W.-F. Elevated-Temperature Space Charge Characteristics and Trapping Mechanism of Cross-Linked Polyethylene Modified by UV-Initiated Grafting MAH. *Molecules* **2020**, *25* (17), 3973.
(42) Qiu, S.; Sun, J.; Li, H.; Gu, X.; Fei, B.; Zhang, S. A green way to simultaneously enhance the mechanical, flame retardant and anti-ultraviolet aging properties of polylactide composites by the incorporation of tannic acid derivatives. *Polym. Degrad. Stab.* **2022**, *196*, No. 109831.
(43) Porfyris, A.; Vasilakos, S.; Zotiadis, C.; Papaspyrides, C.; Moser, K.; Van der Schueren, L.; Buyle, G.; Pavlidou, S.; Vouyiouka, S. Material Behaviour: Accelerated ageing and hydrolytic stabilization of poly(lactic acid) (PLA) under humidity and temperature conditioning. *Polymer Testing.* **2018**, *68*, 315−332.
(44) Islam, M.-S.; Pickering, K.-L.; Foreman, N.-J. Influence of accelerated ageing on the physico-mechanical properties of alkali-treated industrial hemp fibre reinforced poly(lactic acid) (PLA) composites. *Polym. Degrad. Stab.* **2010**, *95* (1), 59−65.
(45) Pluta, M.; Murariu, M.; Alexandre, M.; Galeski, A.; Dubois, P. Polylactide compositions: The influence of ageing on the structure, thermal and viscoelastic properties of PLA/calcium sulfate composites. *Polym. Degrad. Stab.* **2008**, *93* (5), 925−931.

https://doi.org/10.1021/acsomega.3c09296
ACS Omega 2024, 9, 9526−9535